Analysis of the Causes of Differences in Impact Responses between a Human Lower Limb and the Flexible Pedestrian Legform Impactor under Low and High Bumper Vehicle Impact Situations

Takahiro Isshiki, Atsuhiro Konosu, Yukou Takahashi

Abstract The current legform impactors cannot adequately simulate the bending load generated on a lower limb of pedestrians due to the lack of representation of the upper body in a collision with a high-bumper vehicle. It is therefore necessary to develop a new pedestrian legform impact test method applicable for all types of vehicles regardless of the bumper height.

In our previous study, we developed the Simplified Upper Body Part (SUBP) finite element (FE) model, which can represent the upper body by applying it to the human lower limb FE model.

In this study, we attached the SUBP FE model to the flexible pedestrian legform impactor (FlexPLI) FE model then compared it to the SUBP FE model attached to the human lower limb FE model. As a result, the models showed different impact responses. We estimated this was due to the differences between the human lower limb and the FlexPLI. We therefore investigated the main factors of the different impact responses, and clarified the following six improved points to an advanced pedestrian legform impactor to be used for a new pedestrian legform impact test method applicable for all types of vehicles regardless of the bumper height: (1) Mass distribution of the flesh and the long bones, (2) Geometric layout of the ACL and the PCL, (3) Femoral offset, (4) Representation of the ankle joint, (5) Shape of the impact surface of the long bones, (6) Femur bending stiffness.

Keywords pedestrian protection test method, legform impactor, influences of the upper body, computer simulation.

I. INTRODUCTION

Current pedestrian protection test method attempts to assess the protection level of the vehicle structures to the lower limb of a pedestrian by using the legform impactor simulating only the lower limb of a pedestrian. The flexible pedestrian legform impactor (FlexPLI), which is the latest legform impactor applied to the amendment of Regulation No. 127 of the United Nations (UN-R127 Amend.1) [1], has significantly higher biofidelity compared to that of the EEVC pedestrian legform impactor [2], and the FlexPLI is able to evaluate tibia and knee injury risk appropriately for low-bumper vehicles using the maximum values of the bending load generated on a lower limb [3]. However, it has been shown that these current legform impactors cannot adequately simulate the bending load generated on a lower limb of pedestrians due to the lack of representation of the upper body in a collision with a high-bumper vehicle. Recently, in a previous study [4], we found the following: (1) the upper body of a pedestrian significantly influences the bending load generated on the lower limb of a pedestrian, and this influence depends on the bumper height; (2) a compensation for the lack of the upper body by setting the impact height of the FlexPLI 50 mm higher than that of a pedestrian does not work for high-bumper vehicles. It is therefore necessary to develop a new pedestrian legform impact test method that is applicable for all types of vehicles regardless of the bumper height.

Accordingly, in a further study [5] we developed the Simplified Upper Body Part (SUBP) finite element (FE) model, which can take into account the influence of the upper body of a pedestrian by applying it to the human lower limb FE model. As a result, the SUBP can simulate the bending load generated on the lower limb at time historical level, as well as evaluate injury risk not only for the tibia and knee but also for the femur regardless of the bumper height by applying it to a human lower limb. However, it is necessary to conduct the study to apply

T. Isshiki (tel: +81-29-856-0885, e-mail: tissiki@jari.or.jp) and A. Konosu work with the Japan Automobile Research Institute (JARI), Tsukuba, Japan. Y. Takahashi works with the Japan Automobile Manufacturers Association, Inc. (JAMA), Tokyo, Japan.

the SUBP to a legform impactor because the human lower limb cannot be used for a regulatory test.

In this study, we therefore selected the FlexPLI as a base of a legform which can be used for the new pedestrian legform impact test method, then conducted following two analyses. In the first analysis, we attached the SUBP FE model to the FlexPLI FE model then compared its impact responses to that of the SUBP FE model attached to the human lower limb FE model. We found that the models showed different impact responses. Therefore, in the second analysis, we investigated main factors of the different impact responses conducting a sensitivity analysis by changing several constructions of the FlexPLI.

II. METHODS

Computer Simulation FE Models

Figure 1 gives an overview of the computer simulation FE models used in this study. We used the simplified high-bumper vehicle FE model (SUV01), simplified low-bumper vehicle FE model (Sedan01), human lower limb + SUBP FE model, and FlexPLI + SUBP FE model. All simulation analyses were performed with the explicit code PAM-CRASH (ESI Group, France). Regarding impact conditions between the simplified vehicle FE model and the other FE models, we used the same impact conditions between a vehicle and pedestrian targeted in the UN-R127 Amend.1 (impact direction: from the lateral side of a pedestrian, impact speed: 11.1 m/s, impact height: the sole of the foot of a pedestrian is 25 mm above the ground) [1].

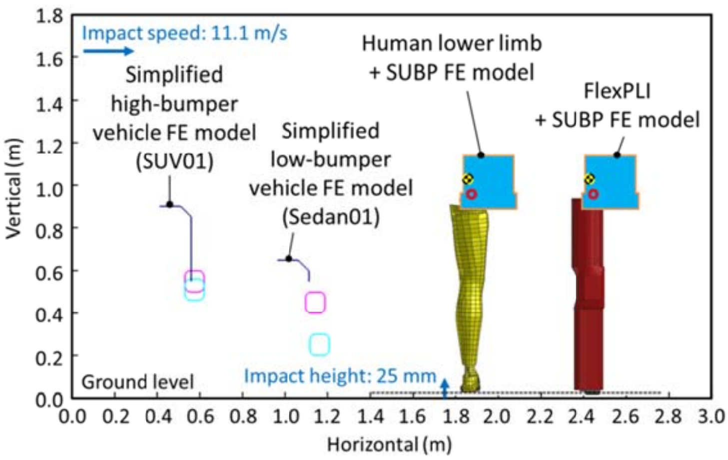

Fig. 1. Overview and impact condition of the computer simulation FE models used in this study.

<u>*Simplified vehicle FE model*</u>: we used the simplified vehicle FE model that was also used in our previous studies [4-5]. In our previous studies, we used a total of 36 simplified vehicle FE models, including a series of 18 simplified high-bumper vehicle FE models and another series of 18 simplified low-bumper vehicle FE models. Regarding the shape of the FE models, we confirmed that the FE models represent a variety of the shape of the production vehicles, by comparing the shape of the FE models to the vehicle shape corridor provided by the International Harmonized Research Activity for Pedestrian Safety (IHRA-PS) working group [6]. Regarding the stiffness of the FE models, the range of the stiffness parameters was estimated from those of different production vehicles, and confirmed that the models generate similar bending loads to the FlexPLI in the same impact configurations [4].

In this study, we used SUV01 and Sedan01 as examples of a high-bumper vehicle and a low-bumper vehicle, respectively. SUV01 shows a representative result among the series of 18 simplified high-bumper vehicle FE models, and Sedan01 shows a representative result among the series of 18 simplified low-bumper vehicle FE models and human full-body FE model impact simulation.

Those two simplified vehicle FE models are composed of three main parts: a Bonnet Leading Edge (BLE), a Bumper (BP) and a Spoiler (SP), as shown in Figure 2. The BLE consists of a deformable shell that simulates the characteristics of a 0.4 mm thick cold rolled steel sheet. This part was designed to reproduce the complicated deformation phenomenon occurring in the BLE of an actual vehicle in longitudinal and vertical directions. The BP and the SP are composed of a combination of a rigid shell tube with a square section connected to a joint element. The joint element restricts motion of the tube to the vehicle longitudinal direction.

Human lower limb + SUBP FE model: we used a human lower limb + SUBP FE model that was developed in our previous study [5]. The human lower limb + SUBP FE model is composed of the human lower limb model and the SUBP model, as shown in Figure 3. The human lower limb model was validated in detail against experimental data obtained with Post Mortem Human Subjects (PMHS) [7-10]. The SUBP model is made by a rigid body and can adequately simulate the influences of the upper body of a pedestrian generated in the lower limb.

A total of ten "injury measures" were output to evaluate the impact responses of the lower limb: bending moment of the femur at three locations (Femur-1 to 3); elongation of the anterior cruciate ligament (ACL); the posterior cruciate ligament (PCL); the medial collateral ligament (MCL) of the knee; and the bending moment of the tibia at four locations (Tibia-1 to 4), as shown in Figure 4. The polarity of the bending moment generated in the femur and the tibia are described in Figure 4. With regards to the polarity of the ACL, the PCL and the MCL injury measure, elongation of the ligaments were defined as positive.

FlexPLI + SUBP FE Model: we used a FlexPLI + SUBP FE model that was developed by replacing the lower limb of the human lower limb + SUBP FE model with the FlexPLI FE model. The FlexPLI FE model has been validated in detail against FlexPLI test data obtained from static and dynamic certifications tests, and has a high fidelity to the actual FlexPLI [11-12]. Ten injury measures were output, as shown in Figure 5. The polarity of the bending moment generated in the femur and the tibia are described in Figure 5. With regards to the polarity of the ACL, the PCL and the MCL injury measure, elongation of the ligaments were defined as positive.

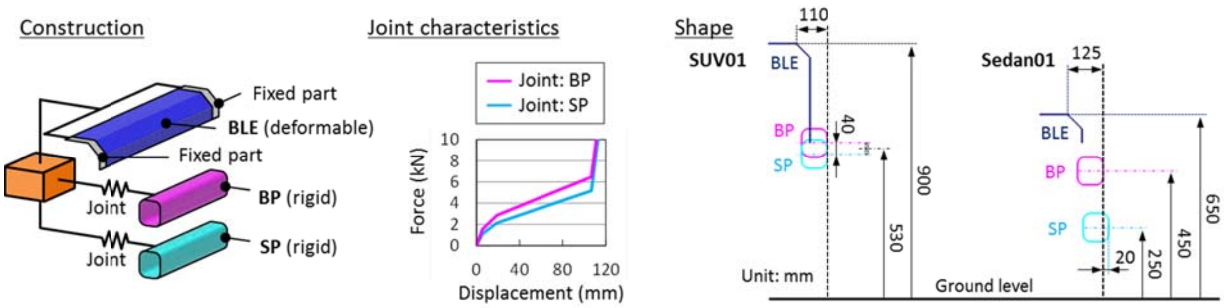

Fig. 2. Simplified vehicle FE models indicating construction, joint characteristics and shape.

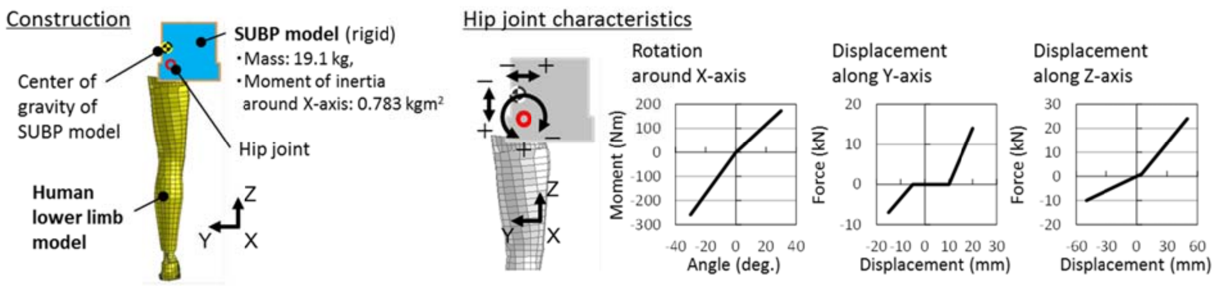

Fig. 3. Human lower limb + SUBP FE model indicating construction and hip joint characteristics.

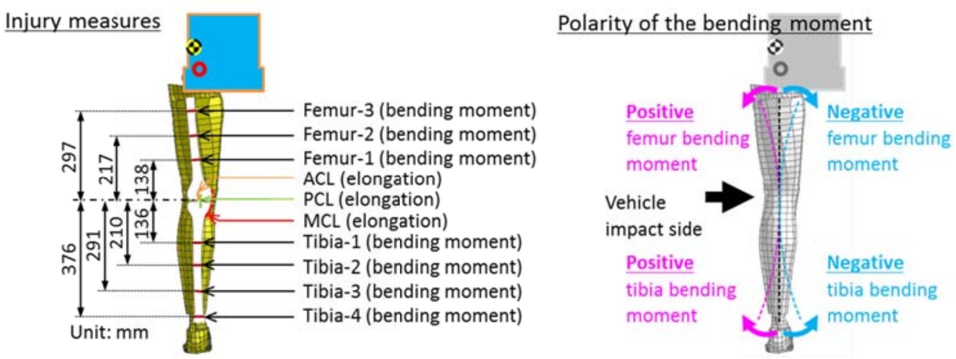

Fig. 4. Human lower limb + SUBP FE model indicating injury measures and polarity of the bending moment.

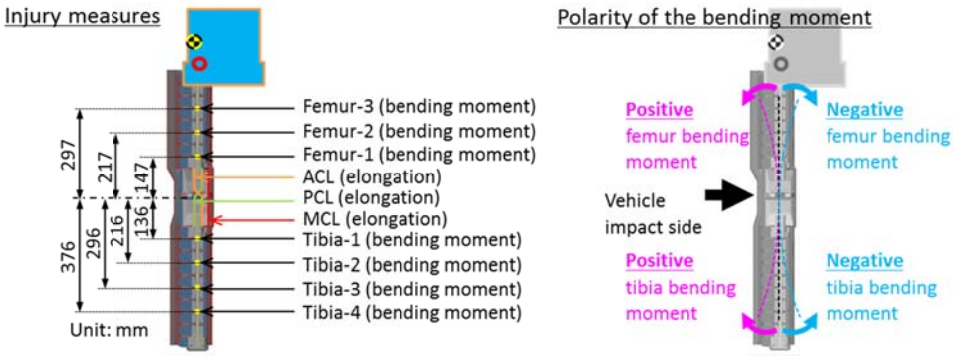

Fig. 5. FlexPLI + SUBP FE model indicating injury measures and polarity of the bending moment.

Analysis 1: Comparison of Impact Responses

In this analysis, to clarify the difference between the FlexPLI and the human lower limb when we attached the SUBP FE model, we compared the maximum values and time histories of injury measures between the FlexPLI + SUBP FE model and the human lower limb + SUBP FE model.

Analysis 2: Main Factors of Difference in Impact Responses

In Analysis 1, the impact responses of the FlexPLI + SUBP FE model showed several differences from those of the human lower limb + SUBP FE model. It is estimated that those differences were caused by the difference in structure between the FlexPLI and an actual human lower limb, because their responses were compared under exactly the same boundary conditions provided by the addition of the same SUBP. Therefore, in this analysis, to obtain an insight into potential improvements of the FlexPLI to develop an advanced pedestrian legform impactor in the future, we investigated the main factors of the differences between the impact responses of the FlexPLI + SUBP FE model and those of the human lower limb + SUBP FE model conducting a sensitivity analysis by changing several constructions of the FlexPLI.

We developed several modified FlexPLI + SUBP FE models, applying six different modifications, as shown in Figures 6–11 respectively, or all at once.

Modification (1) Mass distribution of the flesh and the long bones: the long bones of the FlexPLI are significantly heavier than that of a real human, whereas the flesh of the FlexPLI is significantly lighter than that of a real human. Preceding research has revealed that the difference of mass distribution of the flesh and the long bones significantly affects the vibration of the tibia bending moment [13].

Modification (2) Geometric layout of the ACL and the PCL: the geometric layout of the ACL and the PCL of the FlexPLI do not accord with those of a real human lower limb. This may cause different outputs of the ACL and the PCL elongation of the FlexPLI, compared to that of a human.

Modification (3) Femoral offset: the hip joint of the FlexPLI is located on the femur longitudinal axis, unlike that of a human. This may result in a difference of function of the load from the upper body to the femur top, which would affect the output of the femur bending moment.

Modification (4) Representation of the ankle joint: the FlexPLI does not have an ankle joint (leg and foot are one structure). This may result in a significantly different natural frequency of the leg, which would affect the vibration of the tibia bending moment time histories.

Modification (5) Shape of the impact surface of the long bones: the shape of the impact surface of the long bones of the FlexPLI is different from that of the long bones of a human. This may result in a different contact condition between the vehicle and the lower limb, which would affect the output of the injury measures.

Modification (6) Femur bending stiffness: the femur bending stiffness of the FlexPLI was supposed to be softer than that of a real femur. This may result in a different bending load generated at the femur, as well as other parts of the lower limb, which would affect the output of the injury measures.

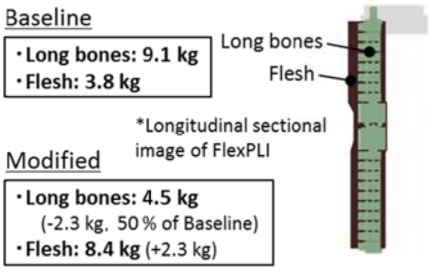

Fig. 6. Modification (1): Mass distribution of the flesh and the long bones.

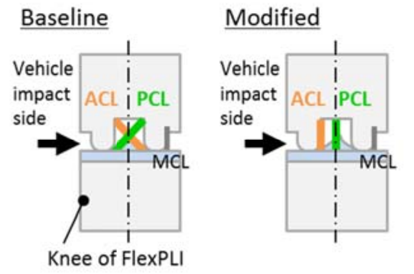

Fig. 7. Modification (2): Geometric layout of the ACL and the PCL.

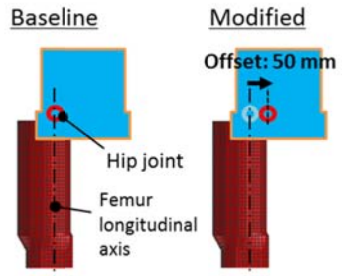

Fig. 8. Modification (3): Femoral offset.

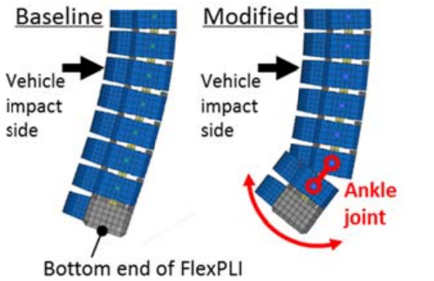

Fig. 9. Modification (4): Representation of the ankle joint.

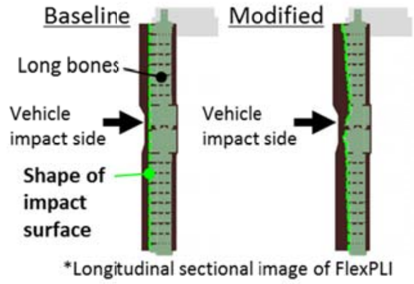

Fig. 10. Modification (5): Shape of the impact surface of the long bones.

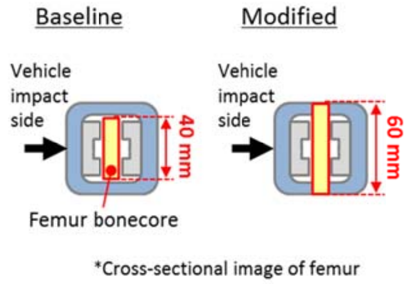

Fig. 11. Modification (6): Femur bending stiffness.

III. RESULTS

Analysis 1. Comparison of Impact Responses

Figure 12 shows the time histories of injury measures obtained from the human lower limb + SUBP FE model and the FlexPLI + SUBP FE model in collision with SUV01 and Sedan01. In this figure, outputs of the FlexPLI + SUBP FE model show several differences compared to those of the human lower limb + SUBP FE model, as follows.

In collision with SUV01:

- Higher vibration of bending moment of Femur-1 and Femur-2 at around 25 ms.
- Smaller values of bending moment of the Femur-2 and Femur-3 at around 30 ms.
- Larger value of the ACL from 20 ms to 55 ms.
- Smaller value of the PCL from 25 ms to 60 ms.
- Higher vibration of the bending moment of Tibia-2, Tibia-3 and Tibia-4 from 25 ms to 45 ms.
- Larger value of the tibia bending moment at around 30 ms and 40 ms.

In collision with Sedan01:

- Higher vibration of the femur bending moment from 10 ms to 30 ms.
- Different mode of the femur bending moment from 30 ms to 60 ms.
- Different mode of the ACL and the PCL elongation from 10 ms to 30 ms.
- Higher vibration of the bending moment of Tibia-1, Tibia-2 and Tibia-3 from 25 ms to 45 ms.
- Second peak exists of the tibia bending moment at around 45 ms.
- Larger value of the bending moment of Tibia-3 at around 10 ms.

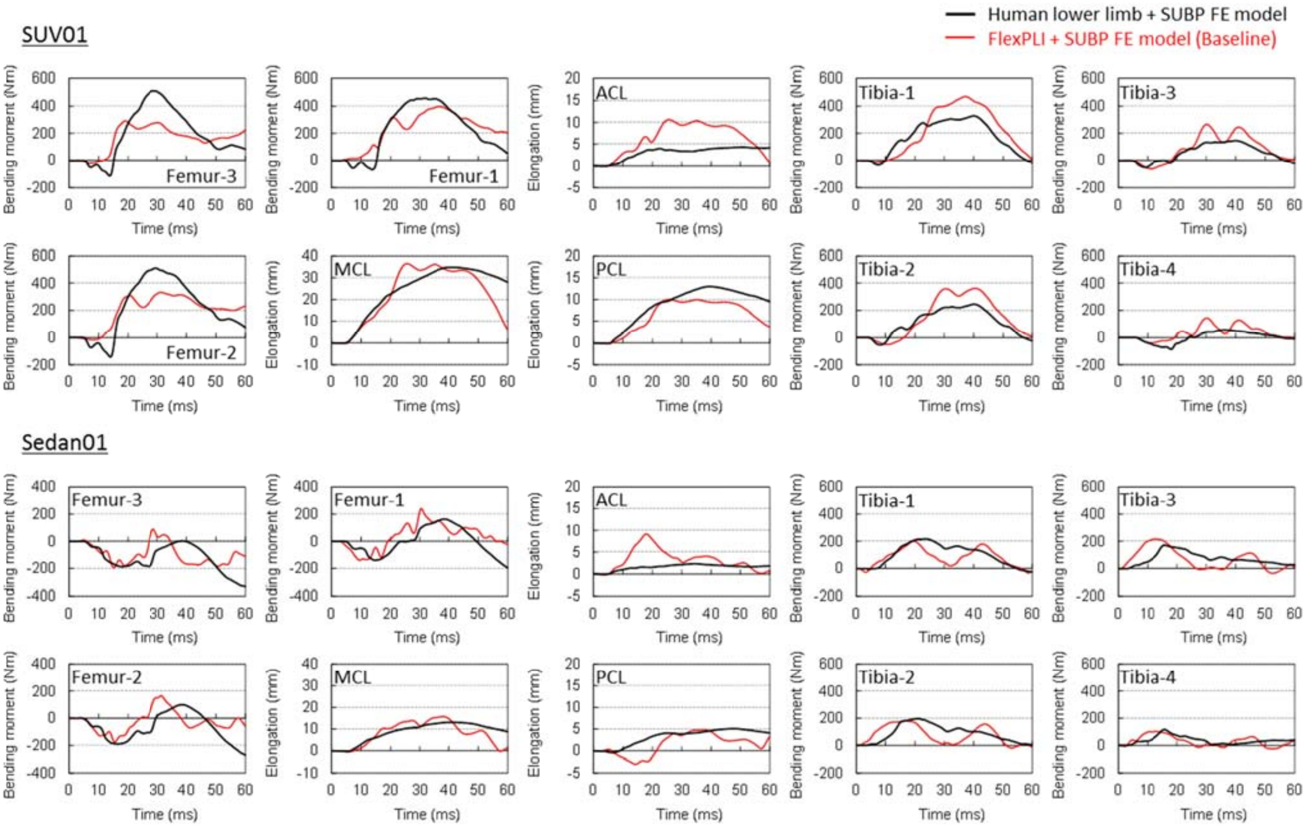

Fig. 12. Injury measure time histories from the human lower limb + SUBP FE model and the FlexPLI + SUBP FE model in collision with SUV01 (*above*) and Sedan01 (*below*).

Analysis 2. Main Factors of Difference in Impact Responses

Figures 13–18 show the time histories of injury measures obtained from the human lower limb + SUBP FE model, the FlexPLI + SUBP FE model (Baseline) and each modified FlexPLI + SUBP FE model in collision with SUV01 and Sedan01. Each modified FlexPLI + SUBP FE model is improved compared to the FlexPLI + SUBP FE model (Baseline), as follows.

Modification (1): Mass distribution of the flesh and the long bones (Figure 13)

In collision with SUV01:

- Higher vibrations of the bending moment of Femur-1 and Femur-2 at around 25 ms are dampened.
- Higher vibrations of the tibia bending moments from 25 ms to 45 ms are dampened.

In collision with Sedan01:

- Higher vibrations of the femur bending moments from 10 ms to 30 ms are dampened.
- Second peak values of the tibia bending moments at around 45 ms are decreased.

Modification (2): Geometric layout of the ACL and the PCL (Figure 14)

In collision with SUV01:

- Larger value of the ACL from 20 ms to 55 ms is decreased.
- Smaller value of the PCL from 25 ms to 60 ms is increased.

In collision with Sedan01:

- Different modes of the ACL and the PCL elongation from 10 ms to 30 ms are reduced.

Modification (3): Femoral offset) (Figure 15)

In collision with SUV01:

- Smaller values of the bending moment of Femur-2 and Femur-3 at around 30 ms are increased.

In collision with Sedan01:

- Different modes of the femur bending moments from 30 ms to 60 ms are reduced.

Modification (4): Representation of the ankle joint (Figure 16)

In collision with SUV01:

- Higher vibrations of the tibia bending moments from 25 ms to 45 ms are dampened.
- Larger values of the tibia bending moments at around 30 ms and 40 ms are decreased.

In collision with Sedan01:

- Larger value of the Tibia-3 bending moment at around 10 ms is improved.

Modification (5): Shape of the impact surface of the long bones (Figure 17)

In collision with SUV01:

- Higher vibrations of the bending moments of Femur-1 and Femur-2 at around 25 ms are dampened.
- Higher vibrations of the tibia bending moments from 25 ms to 45 ms are dampened.
- Larger values of the tibia bending moments at around 30 ms and 40 ms are decreased.

In collision with Sedan01:

- Second peak values of the tibia bending moments at around 45 ms are decreased.

Modification (6): Femur bending stiffness (Figure 18)

In collision with SUV01:

- Smaller values of the bending moment of Femur-2 and Femur-3 at around 30 ms are increased.

Figure 19 shows the time histories of injury measures obtained from the human lower limb + SUBP FE model, the FlexPLI + SUBP FE model (Baseline) and the modified FlexPLI + SUBP FE model (All modifications applied) in collision with SUV01 and Sedan01. The outputs of the modified FlexPLI + SUBP FE model (All modifications applied) are improved for most of injury measures compared to that of the FlexPLI + SUBP FE model (Baseline) for both vehicles qualitatively. Quantitative comparison results are shown in appendix Figure A-1.

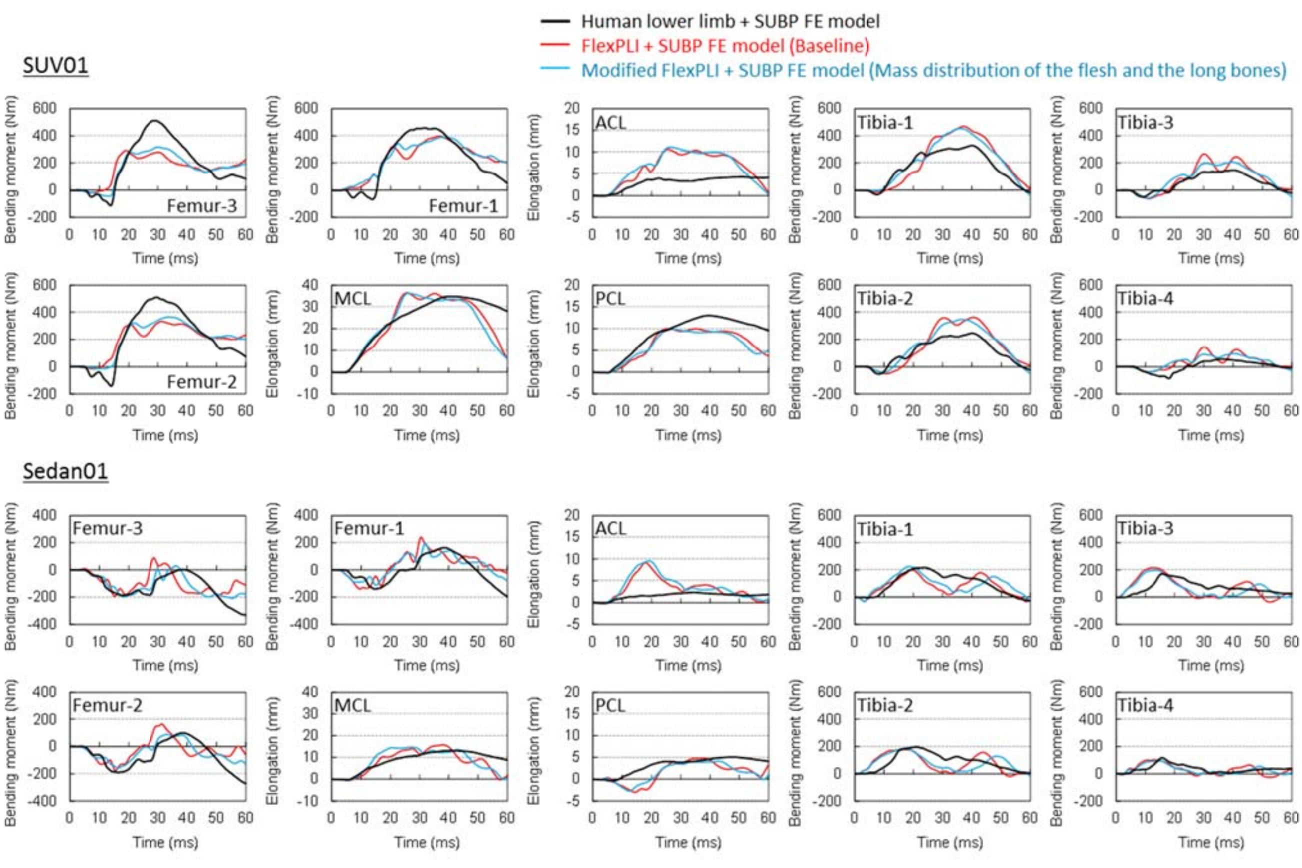

Fig. 13. Time histories of injury measures obtained from the human lower limb + SUBP FE model, the FlexPLI + SUBP FE model and the modified FlexPLI + SUBP FE model *(Modification (1): Mass distribution of the flesh and the long bones)* in collision with SUV01 (*above*) and Sedan01 (*below*).

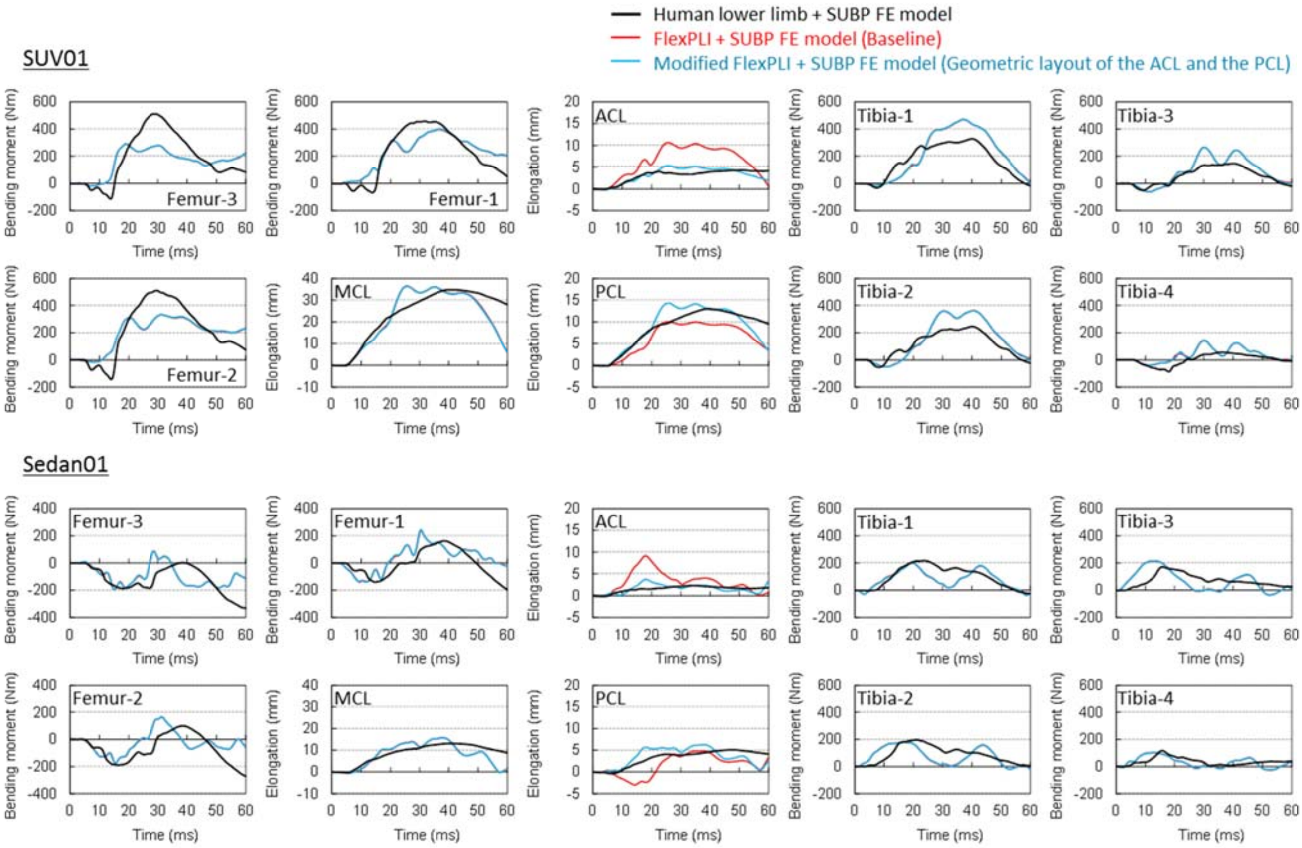

Fig. 14. Time histories of injury measures obtained from the human lower limb + SUBP FE model, the FlexPLI + SUBP FE model and the modified FlexPLI + SUBP FE model *(Modification (2): Geometric layout of the ACL and the PCL)* in collision with SUV01 (*above*) and Sedan01 (*below*).

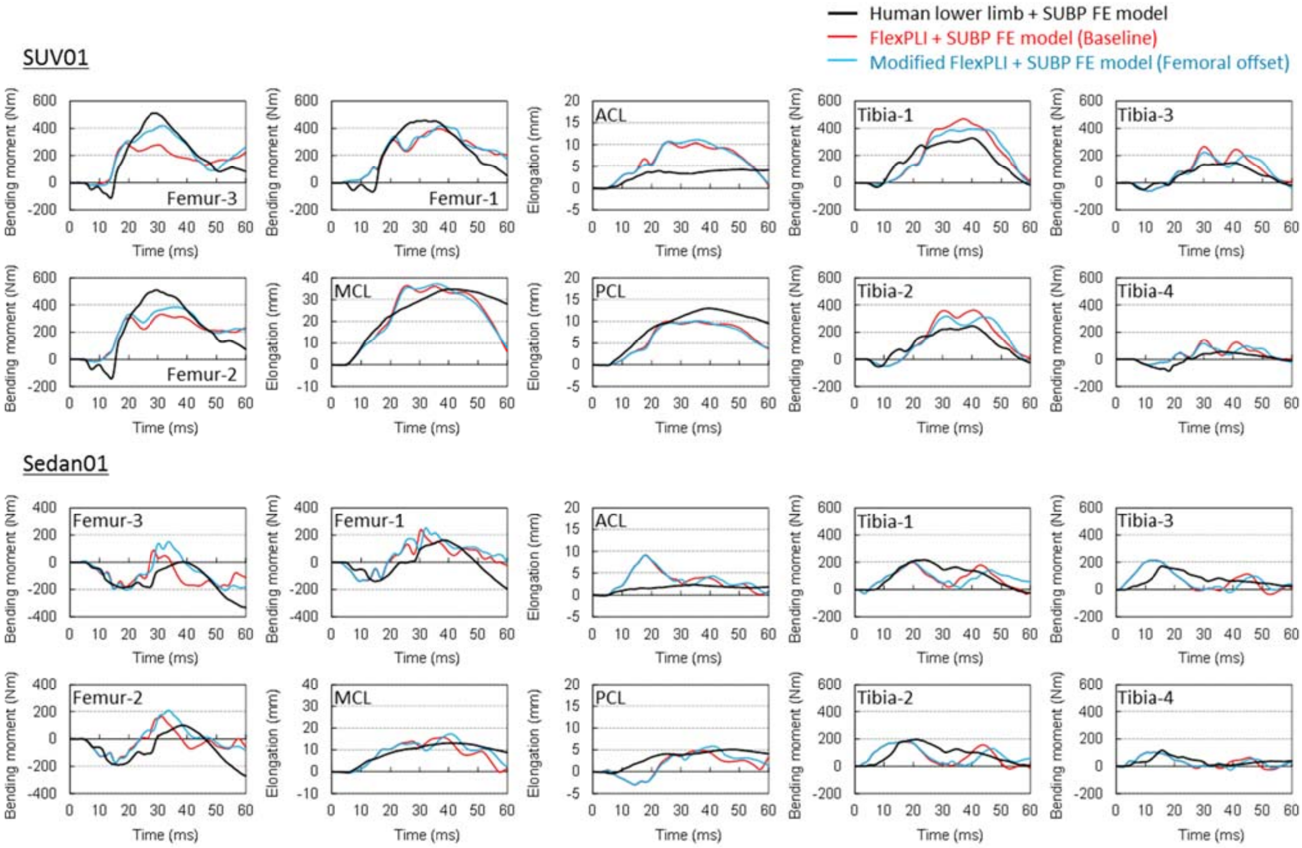

Fig. 15. Time histories of injury measures obtained from the human lower limb + SUBP FE model, the FlexPLI + SUBP FE model and the modified FlexPLI + SUBP FE model *(Modification (3): Femoral offset)* in collision with SUV01 (*above*) and Sedan01 (*below*).

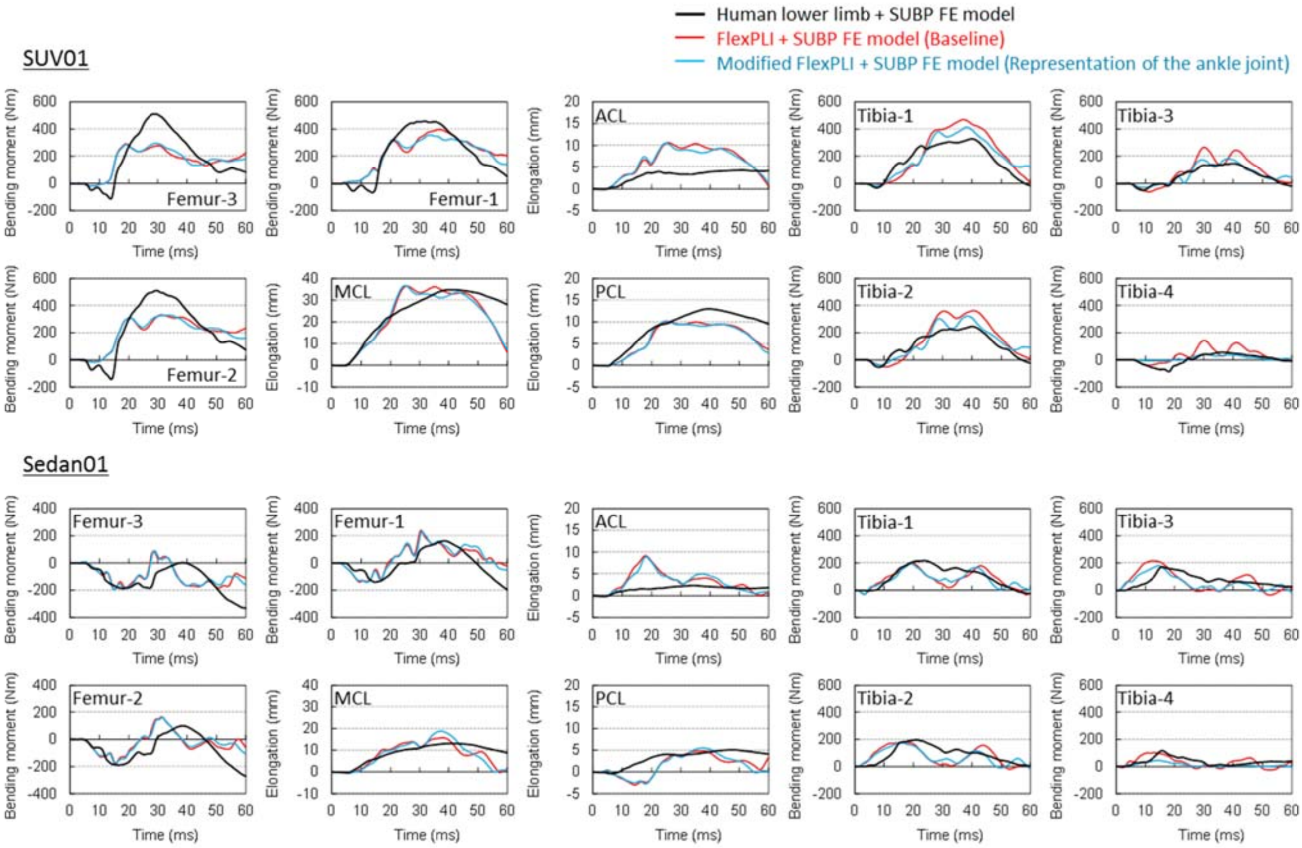

Fig. 16. Time histories of injury measures obtained from the human lower limb + SUBP FE model, the FlexPLI + SUBP FE model and the modified FlexPLI + SUBP FE model *(Modification (4): Representation of the ankle joint)* in collision with SUV01 (*above*) and Sedan01 (*below*).

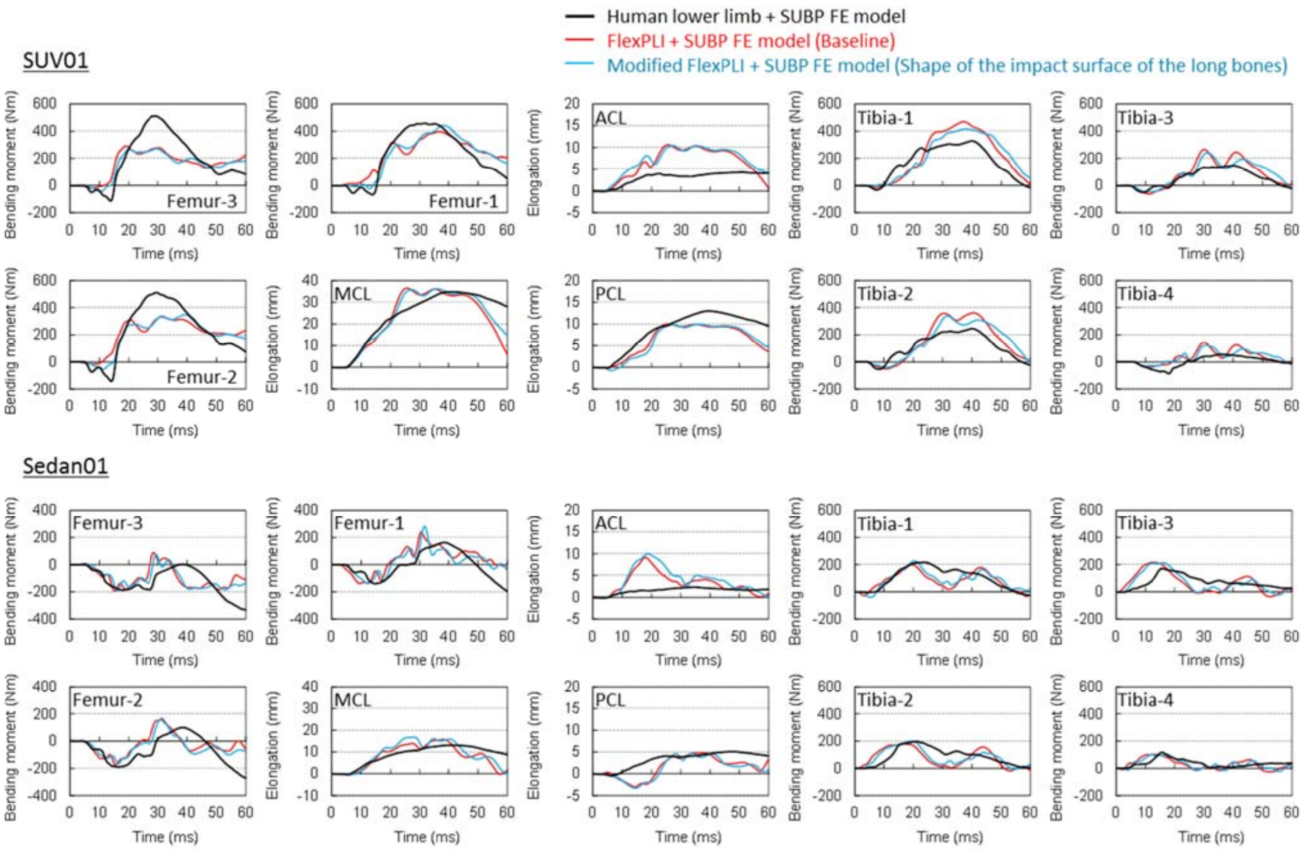

Fig. 17. Time histories of injury measures obtained from the human lower limb + SUBP FE model, the FlexPLI + SUBP FE model and the modified FlexPLI + SUBP FE model *(Modification (5): Shape of the impact surface of the long bones)* in collision with SUV01 (*above*) and Sedan01 (*below*).

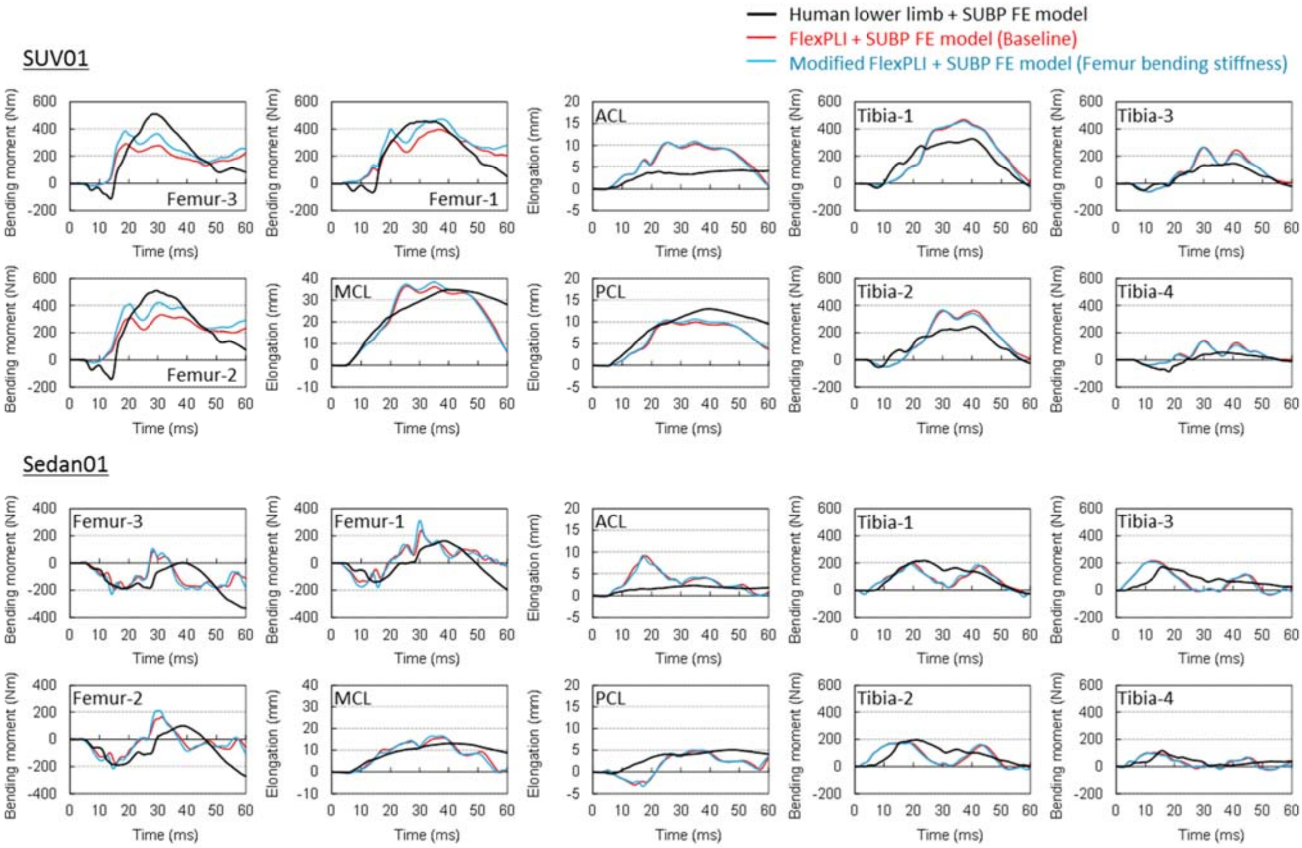

Fig. 18. Time histories of injury measures obtained from the human lower limb + SUBP FE model, the FlexPLI + SUBP FE model and the modified FlexPLI + SUBP FE model *(Modification (6): Femur bending stiffness)* in collision with SUV01 (*above*) and Sedan01 (*below*).

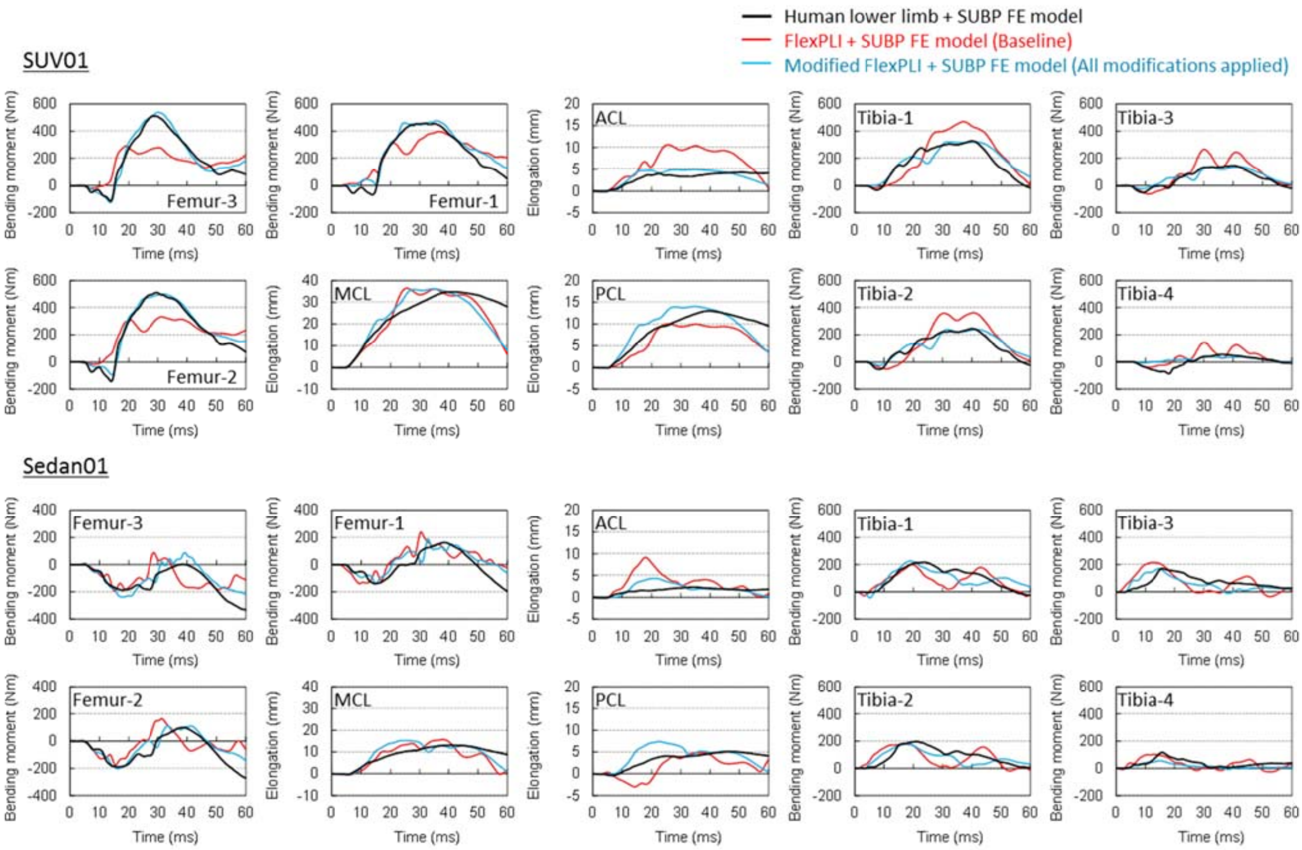

Fig. 19. Time histories of injury measures obtained from the human lower limb + SUBP FE model, the FlexPLI + SUBP FE model and the modified FlexPLI + SUBP FE model *(All modifications applied)* in collision with SUV01 (*above*) and Sedan01 (*below*).

IV. DISCUSSION

In the Analysis 1, it was clarified that the impact responses of the FlexPLI + SUBP FE model show several differences compared with those of the human lower limb + SUBP FE model. The differences were assumed to come from the difference in the structure because the FlexPLI does not exactly represent the structure of a human lower limb due to mechanical constraints.

In the Analysis 2, we therefore conducted sensitivity analysis, changing the construction of the FlexPLI, which were assumed to be the main factors generating the differences. As a result, by comparing the impact responses of the modified FlexPLI + SUBP FE models applying six different modifications respectively with those of the FlexPLI + SUBP FE model (baseline), we were able to find that the following six points clearly affect the impact responses.

Mass distribution of the flesh and the long bones: mass distribution of the flesh and the long bones affects the vibration of the tibia bending mode. Therefore, by making the mass distribution of the FlexPLI closer to that of a human, the vibration of the tibia bending moment was able to be decreased like that of the human lower limb + SUBP FE model.

Geometric layout of the ACL and the PCL: geometric layout of the ACL and the PCL affects the time historical elongation mode. Therefore, by making the layout of the ACL and the PCL closer to that of a human, the difference of the time historical elongation mode with that of the human lower limb + SUBP FE model was able to be decreased.

Femoral offset: as shown in Figure 20, if the offset exists (Human lower limb + SUB FE model case), a force generated along with longitudinal axis of the femur causes a bending moment to apply to the femoral top. On the other hand, if no offset exists (FlexPLI + SUBP FE model (Baseline) case), a force generated along with the longitudinal axis of the femur does not cause any bending moment to apply to the femoral top at all. Therefore, by making the femoral offset of the FlexPLI closer to that of a human, the difference of the bending moment at the femoral top with those of the human lower limb + SUBP FE model was able to be decreased.

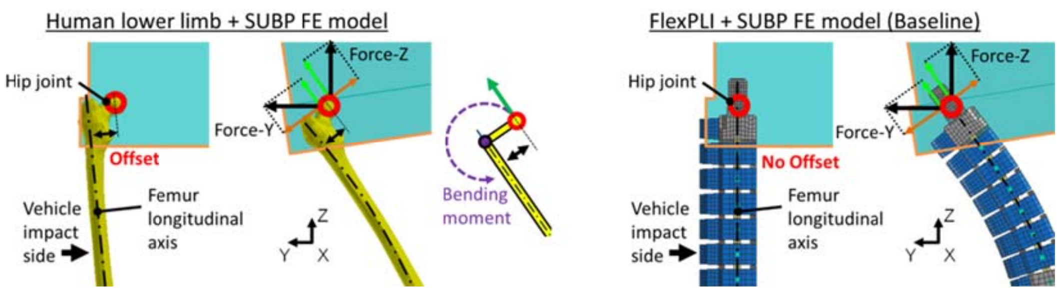

Fig. 20. Mechanism of femoral offset affects the bending moment applied at the femoral top.

Representation of the ankle joint: ankle joint existence affects natural frequency of the lower limb. Therefore, by adding an ankle joint to the FlexPLI, vibration of the tibia can be dampened like that of an actual human.

Shape of the impact surface of the long bones: the shape of the impact surface of the long bones affects the impact situation against the vehicle. Therefore, by making the shape of the FlexPLI closer to that of a human, the bending moment especially generated at the tibia for the low-bumper vehicle impact case and generated at the femur for the high-bumper vehicle impact case can be close to that of a human.

Femur bending stiffness: femur bending stiffness affects the bending load generated at the femur, as well as other parts. Therefore, by making the femur bending stiffness closer to that of a human, outputs of injury measures can be similar to those of a human.

Moreover, by comparing the impact responses of the modified FlexPLI + SUBP FE models applying six different modifications all at once with those of the FlexPLI + SUBP FE model (baseline), we were able to find that the outputs are improved for most of injury measures. We consider that it is necessary to optimize the specifications of the FlexPLI + SUBP FE model using six improved points that clarified in this study as a main parameter to develop an advanced pedestrian legform impactor to be used for a new pedestrian legform impact test method applicable for all types of vehicles regardless of the bumper height.

V. CONCLUSIONS

In this study, we conducted two analyses. In the first analysis, we attached the SUBP FE model, which can simulate the influence of the upper body of a pedestrian to bending load generated on a human lower limb to the FlexPLI FE model then compared its impact responses to that of the SUBP FE model attached to the human lower limb FE model. As a result, the models showed different impact responses. We estimated this was due to the differences in the construction between the human lower limb and the FlexPLI.

In the second analysis, we therefore investigated the main factors of the different impact responses by sensitivity analysis changing the constructions of the FlexPLI, and clarified the following six improved points to an advanced pedestrian legform impactor to be used for a new pedestrian legform impact test method applicable for all types of vehicles regardless of the bumper height: (1) Mass distribution of the flesh and the long bones, (2) Geometric layout of the ACL and the PCL, (3) Femoral offset, (4) Representation of the ankle joint, (5) Shape of the impact surface of the long bones, (6) Femur bending stiffness. We are going to develop an advanced pedestrian legform impactor with above findings as our next step.

VI. REFERENCES

[1] E/ECE/324/Rev.2/Add.126/Rev.1–E/ECE/TRANS/505/Rev.2/Add.126/Rev.1, Regulation No. 127 (01 series of amendments to the Regulation – Date of entry into force: 22 January 2015), Internet: http://www.unece.org/fileadmin/DAM/trans/main/wp29/wp29regs/R127r1e.doc.

[2] GTR9-1-05r1, Informal Group on GTR9 Phase2 (IG GTR9-PH2) 1st Meeting, Technical Discussion – Biofidelity.

[3] Konosu, A., Isshiki, T. and Takahashi, Y. Evaluation of the Validity of the Tibia Fracture Assessment using the Upper Tibia Acceleration Employed in the TRL legform impactor, Proceedings of IRCOBI Conference, 2009, York (UK)

[4] Isshiki, T., Konosu, A. and Takahashi, Y. Influence of the Upper Body of Pedestrians on Lower Limb Injuries and Effectiveness of the Upper Body Compensation Method of the FlexPLI. *Proceedings of 18th International Technical Conference on the Enhanced Safety of Vehicles, Society of Automotive Engineers World Congress*, 2015, Detroit (USA), SAE paper no. 2015-01-1470.

[5] Isshiki, T., Konosu, A. and Takahashi, Y. Development of an Appropriate Pedestrian Legform Impact Test Method which can be used for all Types of Vehicles including High Bumper Vehicles - Development of a Simplified Upper Body Part (SUBP) FE Model. *Proceedings of IRCOBI Conference*, 2014, Berlin (Germany).

[6] Mizuno Y, Chairman, on behalf of IHRA/ P.S. WG. Summary of IHRA Pedestrian Safety WG Activities (2005). Proposed Test Methods to Evaluate Pedestrian Protection Afforded by Passenger Cars, 19th International Technical Conference on the Enhanced Safety of Vehicles, 2005, Washington, D.C. (USA), paper no. 05-0138.

[7] Takahashi, Y., Kikuchi, Y., Mori, F. and Konosu, A. Advanced FE lower limb model for pedestrians. *Proceedings of 18th International Technical Conference on the Enhanced Safety of Vehicles*, 2003, Nagoya (Japan), paper no. 03-0218.

[8] Takahashi, Y., Kikuchi, Y. and Mori, F. Development of a finite element model for a pedestrian pelvis and lower limb. *Society of Automotive Engineers World Congress*, 2006, Detroit (USA), SAE paper no. 2006-01-0683.

[9] Kikuchi, Y., Takahashi, Y. and Mori, F. Full-scale validation of a human FE model for the pelvis and lower limb of a pedestrian. *Society of Automotive Engineers World Congress*, 2008, Detroit (USA), SAE paper no. 2008-01-1243.

[10] Takahashi, Y., Suzuki, S., Ikeda, M. and Gunji, Y. Investigation on pedestrian pelvis loading mechanisms using finite element simulations. *Proceedings of IRCOBI Conference*, 2010, Hanover (Germany).

[11] UN/ECE/WP29/GRSP/INF-GR-PS/Flex-TEG 2009. Development of a FE Flex-GTR-prototype model and Analysis of the Correlation between the Flex- GTR-prototype and Human Lower Limb Outputs, TEG-096, http://www.unece.org/fileadmin/DAM/trans/doc/2009/wp29grsp/teg-096e.pdf.

[12] Issiki, T., Konosu, A. and Tanahashi, M. Development of an FE biofidelic flexible pedestrian leg-form impactor (Flex-GTprototype) model. *20th International Technical Conference on the Enhanced Safety of Vehicles*, 2007, Lyon (France), Paper Number 07-0179.

[13] Takahashi, Y., Imaizumi, I., Asanuma, H. and Ikeda, M. Responses of the Flexible Legform Impactor in Car Impacts. *Proceedings of IRCOBI Conference*, 2013, Gothenburg (Sweden), pp. 777–88.

VIII. Appendix

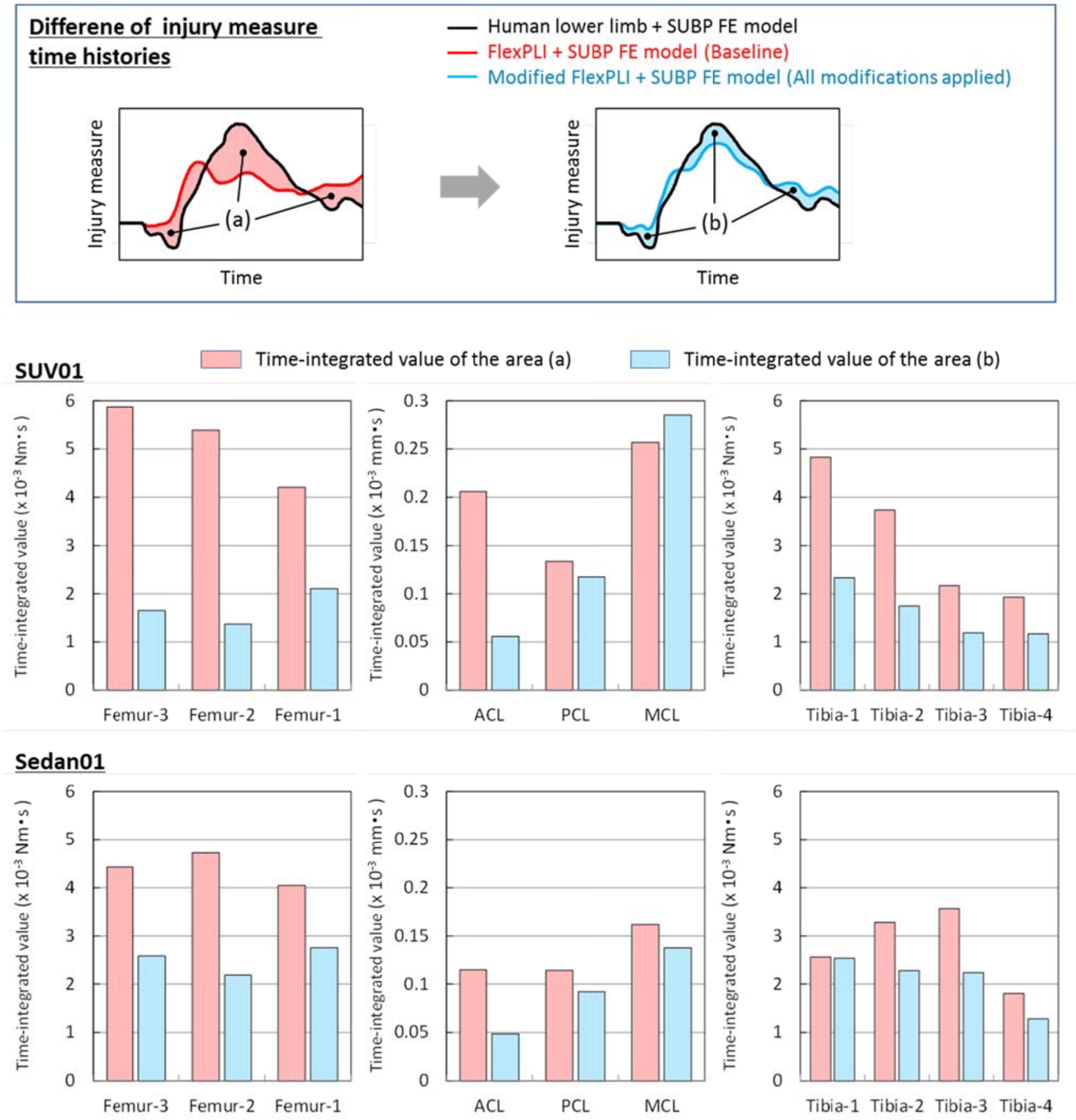

Fig. A-1. Differences of the injury measure time histories between the human lower limb + SUBP FE model and the FlexPLI + SUBP FE models.